Journal Pre-proof

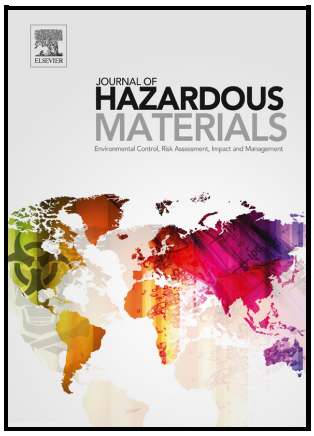

Assessing indicators of arsenic toxicity using variable fluorescence in a commercially valuable microalgae: physiological and toxicological aspects

Shagnika Das, Fabrice Lizon, François Gevaert, Capucine Bialais, Gwendoline Duong, Baghdad Ouddane, Sami Souissi

PII: S0304-3894(23)00497-1

DOI: https://doi.org/10.1016/j.jhazmat.2023.131215

Reference: HAZMAT131215

To appear in: *Journal of Hazardous Materials*

Received date: 8 December 2022
Revised date: 17 February 2023
Accepted date: 13 March 2023

Please cite this article as: Shagnika Das, Fabrice Lizon, François Gevaert, Capucine Bialais, Gwendoline Duong, Baghdad Ouddane and Sami Souissi, Assessing indicators of arsenic toxicity using variable fluorescence in a commercially valuable microalgae: physiological and toxicological aspects, *Journal of Hazardous Materials,* (2023) doi:https://doi.org/10.1016/j.jhazmat.2023.131215

Assessing indicators of arsenic toxicity using variable fluorescence in a commercially valuable microalgae: physiological and toxicological aspects

Shagnika Das[1*], Fabrice Lizon[1], François Gevaert[1], Capucine Bialais[1], Gwendoline Duong[1], Baghdad Ouddane[2], Sami Souissi[1]

[1] Univ. Lille, CNRS, Univ. Littoral Côte d'Opale, IRD, UMR 8187 – LOG - Laboratoire d'Océanologie et de Géosciences, Station marine de Wimereux, F-59000 Lille, France.

[2] Univ. Lille, CNRS, UMR 8516 – LASIRE - Equipe Physico-chimie de l'Environnement, Bâtiment C8, F-59000 Lille, France.

Highlights-

1. Arsenic (As) enhanced photoprotective processes and restricted biomass production.
2. Optical and functional absorption cross-section are useful indicators of As toxicity.
3. Non-photochemical quenching (NPQ-NSV) positively correlated to de-epoxidation ratio.
4. Significant affinity between Fe and As bioaccumulation by *D. lutheri* was observed.
5. Variable fluorescence endorsed an easy and compliant method to show As toxicity.

Abstract-

Indicators signaling Arsenic (As) stress through physiology of microalgae using non-destructive methods like variable fluorescence are rare but requisite. This study reports stress markers indicating arsenic (As) toxicity (in two concentrations 11.25 µg/L and 22.5 µg/L compared to a control) exposed to a microalga (*Diacronema lutheri*), using fast repetition rate fluorometry (FRRf). Growth and physiological parameters such as cell density, chl *a* and the maximum quantum yield F_v/F_m showed coherence and impeded after the exponential phase (day 9 - day 12) in As treatments compared to the control ($p < 0.05$). On contrary photo-physiological constants were elevated showing higher optical (a_{LHII}) and functional [Sigma (σ_{PSII})] absorption cross-section for the As treatments ($p < 0.05$) further implying the lack of biomass production yet an increase in light absorption. In addition, As exposure increased the

energy dissipation by heat (NPQ-NSV) showing a strong relationship with the de-epoxidation ratio (DR) involving photoprotective pigments. Total As bioaccumulation by *D. lutheri* showed a strong affinity with Fe adsorption throughout the algal growth curve. This study suggests some prompt photo-physiological proxies signaling As contamination and endorsing its usefulness in risk assessments, given the high toxicity and ubiquitous presence of As in the ecosystem.

Keywords - *Diacronema lutheri*, Arsenic bioaccumulation, Optical absorption cross section, pigment concentrations, de-epoxidation ratio (DR).

Environmental implication

Arsenic is ubiquitous and hazardous to human health in trace amounts, given the dreadful record of lethal cases from arsenic contamination, worldwide. Hence, new tools are warranted for this compelling necessity to monitor effects of arsenic in nature. This study proposes new indicators of arsenic contamination through physiology of a microalgae (*Diacronema lutheri*) using variable fluorescence. Furthermore, a linkage of physiological markers with ecotoxicology using non-destructive, rapid and a precise method is reported. A strong correlation of variable fluorescence and growth parameters exemplified the precision of the proposed indicators. Such rapid, non-polluting, novel techniques are advantageous to environmental risk assessors.

1. Introduction

Trace metal contamination has posed serious threats to aquatic and terrestrial organisms since the time of heavy industrialisation and globalisation (Chiellini et al., 2020; Das et al., 2022a) . Some trace metals prove to have essential roles in the metabolism of organisms, but only up to a certain concentration, beyond which, it is often toxic (Zidour et al., 2019; Kadiene et al., 2019; Das et al., 2019; Das et al., 2020b). Arsenic (As) is one such element that shows no

evidence for its essentiality in functioning of organisms and has been globally regarded as a serious threat to life in general, from microbes to mammals (Morelli et al., 2005; Hussain et al., 2021; Xiao et al., 2022). It is often described as a ubiquitous metal that can originate from anthropogenic, geo-genic and/or natural pathways like erosion of soil, volcanic eruptions, etc. (Z. Wang et al., 2020) . Industries such as fossil fuel, agricultural factories using arsenic based pesticides, smelting or metal extraction factories are some examples of the man-made sources of As (Morelli et al., 2005; Rathi and Kumar, 2021). In comparison to terrestrial animals, marine organisms have higher load of total As concentration ranging from 1-1000 µg/g in dry weight which is almost 100 times more than land creatures ranging from 0.1 -10 µg/g in dry weight (Cima et al., 2003; Duncan et al., 2015).

Being the primary producer of the marine ecosystem, phytoplankton are often the earliest or the primary target that bear the consequences of arsenic toxicity in marine coastal areas, which are often perceived as heavily impacted zones due to the active commercial and industrial pursuits for decades (Aboal et al., 2022; Duncan et al., 2015). Marine algal species forms the basis of the trophic energy flow of the ecosystem and has profoundly proved its role as great indicators of the health of an ecosystem in many ecotoxicological studies (Martins et al., 2015; Gan et al., 2019; Hussain et al., 2021; Li et al., 2021; Das et al., 2022a). Previous literatures concerning algal toxicity, have laid theories and explanation on the processes adapted by marine algae to combat the incessant exposure to arsenic, discussing the detoxification pathways, bio-transformation of metal states, etc. (Hasegawa et al., 2001; Morelli et al., 2005; Grotti et al., 2010; Maher and Eyre, 2011; Duncan et al., 2015). Biotransformation is the process that involves uptake of inorganic metal forms which then is either oxidized, reduced or methylated to organic states through an algal cell or other organisms (Zhang et al., 2022). Such studies mostly reflected the changes in the growth rate, pigment contents, morphological changes, biochemical alterations, and

bioaccumulation capacity highlighting on metabolic activities and population structure (Costa et al., 2019; Li et al., 2021; Hussain et al., 2021; Das et al., 2022a). However, the effect of trace metal exposure and its consequences on the photosynthetic machinery and the associated physiological variables of an alga has not been much explored in the literature and such reports can shed light on valuable physiological indicators when exposed to metal stress. Variable fluorescence (VF) is such a technique that can be used for assessing physiological condition/state of the algal photosynthetic apparatus often used in studies related to limnology and laboratory cultures (Schallenberg et al., 2020; Ryan-Keogh and Thomalla, 2020; Schuback et al., 2016; Schuback et al., 2020). However, variable fluorescence can also be used in the detection of toxicity or any form of stress providing prompt and efficacious physiological indicators to evaluate the risk factors prevailing in the marine habitats (Suresh Kumar et al., 2014; Banks, 2018; Gan et al., 2019; Beaulieu et al., 2020). This technique makes it possible to study in a non-intrusive way the efficiency of the photosynthetic processes of microalgae, *in situ* natural environment or in experiments whether or not related to water quality issues. The key parameters concerning the functioning of the photosynthetic apparatus used in previous studies were: the maximum quantum yield (Fv/Fm) of photochemistry in photosystem II (PSII), the maximum electron transport rate (ETRmax) in relative (rETRmax) or absolute units (ETRmax(II)), the absorption cross section of PSII photochemistry (σ_{PSII}) and the non-photochemical quenching (NPQ) (Suresh Kumar et al., 2014; Huang et al., 2015; Gan et al., 2019; Beaulieu et al., 2020). Identification of new indicators specific to highly toxic contaminants like arsenic can assist the environmental management and risk assessment groups to analyse the varied threats posed on the marine ecosystem with much rapidity and precision by using variable fluorescence methods for stress physiology (Gan et al., 2019).

In this work, we studied the marine algal species *Diacronema lutheri*, characterised with phytosterol richness and a variety of mostly type A pigments (chla, c1, chlorophyllides) with two dissimilar (in length) flagella (Ahmed et al., 2015; Das et al., 2022a). *Diacronema lutheri* is an eco-friendly source for producing valuable compounds like phytosterol due to its natural richness and is also majorly used in the sector of aquaculture especially as a feed for bivalves, copepods which in turn are fed to fish larvae, shrimps in farms and other cultured organisms, making it ecologically and economically valuable (Carvalho et al., 2009 ; Das et al., 2017; Das et al., 2020a). Previous literatures reported that *D. lutheri* is a bioindicator species, signalling stress from trace metals by lowering photosynthetic pigment, cell density and by exemplifying capacity of bioaccumulating and bioconcentrating varied amount of essential and non-essential trace metals (Das et al., 2022a). In this study our objective was to comprehend the physiological anomalies caused due to arsenic exposure in *D. lutheri* using the variable fluorescence technique through Fast Repetition Rate fluorometer (FRRf) in linkage with pigment analyses by high-performance liquid chromatography (HPLC). Thus, the goal is not only to characterize the impact of toxic metal on physiology of this species but to have a functional understanding of the phenomenon of toxicity. The VF technique was implemented to compare the photosynthetic processes occurring in photosystem II (PSII) apart from which the monitoring of cell density, pigment contents and the bioaccumulation capacity of *D. lutheri* was also analysed in control group and arsenic-exposed algal cells. In natural environments, a complex and often a cocktail of metal exists and previous studies reported that such coexistence of multiple trace metals can influence the toxicity and/or the absorption of metals in the body of the organisms, such as Iron (Fe) or Manganese (Mn) oxides influence the mobility of As. Hence, a range of trace metals were studied in order to comprehend the bioaccumulation of other trace metals apart from As (Carneiro et al., 2022; (Anawar et al., 2018). Hence, studies on such issues are warranted for the rapidity to detect

As contamination which can further aid on the risk assessment of utilising such ecologically and economically important algal species in the medicinal or aquaculture farms, concerning the pollutants present in the environment.

2. Material and methods

2.1 Test organism- *Diacronema lutheri*

The initial stock of the microalgae *D. lutheri* was acquired from the Roscoff Culture Collection in France (RCC-1537). Laboratory cultures were then initiated in 6 L flasks using artificial seawater prepared from osmosed water and artificial salt (coral salt-pro). All the cultures were maintained under controlled laboratory conditions in an incubator with a 12h: 12h light/dark regime at 18° C with salinity 33. The cultures were supplemented or enriched by adding vitamins and the Conway medium (Tlili et al., 2016; Arias et al., 2017; Gnouma et al., 2017). The preparation of Conway medium was done by following previous studies (Tlili et al., 2016; Arias et al., 2017; Das et al., 2022a).

2.2 Exposure to Arsenic (As)

The exposure of As to *D. lutheri* was executed in 6 L sterilised flasks in controlled laboratory set-up similar to that of the culture conditions. A lower and a higher value of As concentration (environmentally realistic) was used in this study, which were, 11.25 µg/L; and 22.5 µg/L. Our study followed the entire algal growth curve and reported the alterations in the photosynthetic machinery in link with the pigment contents. The experiment was carried out with the two concentrations of As exposure and a control treatment with each treatment containing three replicates (n = 3).

2.3 Experimental set up and cell counts

Algal cells from the sterilised culture were passed on to the experimental flasks of 6 L along with Conway medium and vitamins on the first day of the experiment (T0) comprising of 0.5 $\times 10^6$ cells/mL following the guidelines of the initial concentration for biomass reported in Organization for Economic Cooperation and Development (OECD, 2011). To observe the growth curve of *D. lutheri*, 2 ml samples from each treatment and replicate was taken in Eppendorf tubes, fixed with 5 % lugol solution and stored at 4° C until analysis (Arias et al., 2017) . The cell density of each condition was recorded with the help of an inverted microscope (Olympus, IX 71, Tokyo, Japan) in triplicates by observing the cells on a Malassez cell slide (haemocytometer, 0.1mm depth, Japan) by following the same protocol described in (Das et al., 2022) . The entire growth curve of *D. lutheri* was followed from day 0 (T0) until day 21 (T21) intermittently every 3 days.

2.4 Trace metal analysis

An inductive coupled plasma atomic emission spectrometer (Agilent 5110 SVDV ICP-OES, United States) was used for all the analyses of trace metals in the algal biomass and in the residual water of the exposed medium along with the control. The algal biomass was collected on sterile membrane filters of size 0.45 micron and diameter of 47 mm with the help of a filtration system. These filters collected from all the replicates of each treatment were dried in a desiccator and the dried filters were then subjected to acid digestion with nitric acid (HNO_3) and hydrochloric acid (HCl) mixed in the ratio of 1:3 in Teflon tubes. In each tube a final volume of 5 mL double distilled (MilliQ) ultrapure water was added and then analysis for trace metal concentration with ICP-OES was done. For the residual metal concentrations in the filtrate, water samples were collected in falcon tubes (15 mL) from all the experimental conditions, fixed with 20 µL of ultrapure HNO_3 and kept in dark until further analysis under ICP-OES without any required pre-treatment. The entire trace metal analysis and the conservation of the quality of each element or standard solution utilised

during this experiment was optimally maintained and a multi-elemental standard for trace metal analysis was exerted as a reference for the identified trace metals (Ouddane, 1990; Das et al., 2023). Trace metal values and analyses were validated by using Certified Reference Materials (CRM) HISS-1 and PACS-3. A good concurrence between certified estimates and the one obtained with the ICP was observed with ≤10% total analytical errors during all the metal mineralization procedures.

2.5 Analysis of algal physiology by variable fluorescence

Variable fluorescence (VF) was studied here through the FRRf that was regulated with an Act2-based laboratory system (Chelsea Technologies Group Ltd, UK) using a FastOcean sensor. Measurements were realized on diluted samples (1:9 of medium, due to very high biomass concentrations) collected at a specific time and order every three days until T21, from each treatment and replicates to avoid any variability. The acquisition protocol for VF measurements was the classical single-turnover (ST) protocol as described by (Aardema et al., 2019) for instance. It consisted of 120 excitation flashes with a flash pitch of 2 μs and 40 relaxation flashes with a flash pitch of 60 μs. Excitation flashes were performed only with the blue LED (450 nm) for this study since chlorophyll *a* (chl *a*) was the main photosynthetic pigment of our strain. Fluorescence rises were parametrized with the classical model (Oxborough et al., 2012) directly with the Act2RUN Software, which also allows to derive the Sigma PSII parameter (σ_{PSII} in nm^{-2} $PSII^{-1}$) corresponding to the functional absorption cross section of PSII. From this two fluorescence rise measurements, the maximum (F_v/F_m, dimensionless) and the effective (F_q'/F_m', dimensionless) quantum efficiency of photosystem II (PSII) were respectively calculated as:

$$\mathbf{F_v / F_m = (F_m - F_0)/F_m} \quad \text{Eq (1)}$$

$$\mathbf{F_q' / F_m' = (F_m' - F')/ F_m} \quad \text{Eq (2)}$$

The absolute PSII photochemical flux was calculated for each light step (E) according to the so-called "absorption-algorithm" of (Oxborough et al., 2012), commonly used in aquatic systems (Aardema et al., 2019; Serre-Fredj et al., 2021) and for experiments in laboratories (Gan et al., 2019). This PSII flux is a volume-specific PSII photochemical flux, also called JVPII (µmol electrons m^{-3} s^{-1}), which is an important step in calculating primary production of microalgae (Schuback et al., 2021a) rather than the "Sigma algorithm" (also called JPII). JVPII is the product of the effective PSII efficiency previously described (F_q'/F_m'), the optical absorption cross section of the light harvesting pigments of PSII (a_{LHII} in m^{-1}) and the irradiance E (µmol photon m^{-2} s^{-1}):

$$\mathbf{JVPII} = (\mathbf{F_q'/F_m'}) \times \mathbf{a_{LHII}} \times \mathbf{E} \quad \text{Eq (3)}$$

$$\mathbf{a_{LHII}} = [(\mathbf{F_0} \times \mathbf{F_m}) \div (\mathbf{F_m} - \mathbf{F_0})] \times \mathbf{K_a} \quad \text{Eq (4)}$$

The parameter K_a (m^{-1}) is an instrument specific factor necessary for obtaining the volumetric and absolute rate of electron transport JVPII according to the algorithm of Oxborough et al., 2012 .

Computed JVPII versus light E were then fitted by a classical model (Eilers and Peeters, 1988) with the phytotools R package (Brunet et al., 2014) , in order to derive photosynthetic parameters such like the absolute light utilization efficiency (α_{II} in µmol electrons (µmol photons)$^{-1}$, the initial slope of the FLC) for each samples and experimental conditions (Falkowski and Raven, 2013).

For each condition and light steps, a measure of non-photochemical energy dissipation was also calculated with the normalized Stern-Volmer quenching coefficient (NPQ-NSV, McKew et al., 2013) from the fluorescence rise parameters as:

$$\mathbf{NPQ - NSV} = \mathbf{F_0'/F_m'} \quad \text{Eq (5)}$$

where F_0' was estimated according to Oxborough and Baker, 1997 as $F_0' = F_0/ (F_v/F_m + F_0/F_m')$ and $F_v' = (F_m' – F_0')/F_m'$. For this study, only values at high light intensity (E = 800 µmol photon m^{-2} s^{-1}) are displayed because they were the most efficient to discriminate the different experimental conditions. Finally, we compute 1/Tau' (in the light regulated state, in ms^{-1}), as the rate of re-opening of closed reaction centres of PSII (RCII). 1/Tau' was derived from the relaxation phase of the ST fluorescence rise by fitting an exponential decay curve to the data using ACT2RUN software (as for the excitation phase fit). We displayed here averaged values of 1/Tau' measurements consistent with the light intensity of culture condition (that is to say for 3 low light steps of the FLC: E = 48, 106 and 176 µmol photon m^{-2} s^{-1}). A detailed section of the material and methods (section 1S: Table 1S, 2S and 3S) was added along with a flow chart of the entire process of VF measurements (Fig. 1S)

2.6 Pigment analysis

The samples for the pigment concentrations in *D. lutheri* were obtained by filtering the algae from each treatment and replicate on GF/F Whatman filters in dark and were stored in -20°C for not more than three weeks before the analysis. The filters were compressed by using a grinder in order to extract the pigments with methanol followed by 30 µL drop-wise additions of methylene chloride. Membrane filters of Polytetrafluoroethylene (0.45µm) were used to filter the extracts which were further concentrated by using a stream of nitrogen gas. The extract for the pigment analysis was then subjected to salt removal by a 50:50 volume/volume mixture of distilled water and methylene chloride. The organic portion of the extract was further concentrated by dry evaporation with nitrogen gas. An addition of solvent (40 µL of methanol) was done before analysis, from which 20 µL were injected in a High-Performance Liquid Chromatography (HPLC, Shimadzu, Nexera XR provisioned with a C18 reverse-phase column, Allure, Restek) instrument and the analysis of pigment concentration was enforced by following a solvent delivery profile adapted from Arsalane et al., 1994 . In

addition to chlorophyll *a* content, the de-epoxidation ratio (DR) was calculated as the ratio of the photoprotective pigments that are involved in the xanthophyll cycle to denote any possible stress response that triggered in the algal cells when exposed to As by following equation (6) (Brunet et al., 2014; Ji et al., 2018 ; Das et al., 2022a):

DR = Diatoxanthin / (Diadinoxanthin + Diatoxanthin) ..... Eq (6)

2.7 Statistical analysis

All the physiological parameters like F_v/F_m , Sigma (σ_{PSII}), a_{LHII}, 1/Tau', NPQ-NSV and the pigment chl *a* along with algal cell density in each treatment including the control were compared by analysis of variance (ANOVA) at $p < 0.05$, after meeting all the requirements of normality and homogeneity of variance. To test the normality and the homogeneity a Shapiro Wilk normality test and a Levene's Test for Homogeneity of Variance were carried out respectively. To compare the significance in each condition Tukey multiple comparisons of means (95% family–wise confidence level) was applied to the data. The linear regression between NPQ-NSV and the de-epoxidation ratio was done by using Pearson's correlation at $p < 0.05$. The analyses were accomplished with R studio (4.0.4).

3. Results

3.1 Biomass of *D. lutheri*

3.1.1 Chlorophyll *a* content and growth curve of *D. lutheri*

Chl *a* content displayed on Fig.1 (control, As (11.25 µg/L) and As (22.5 µg/L)) measured at each interval of time from T3 until T21 shows an initial increase and then a declination in all

the treatments. The chl *a* increased from T3 to T9 significantly for control ($p < 0.05$). The treatment As (11.25 µg/L) increased chl *a* from T3 to T9 and further to T15 significantly (<0.01). Lastly, for the treatment As (22.5 µg/L) increased chl *a* significantly from T3 to T15. At the lysis phase no significant reduction in the chl *a* content was observed for control at T21 from T9, however, chl *a* reduced significantly in both the As exposed treatments at T21 from T15. In between the treatments, the control showed significantly higher chl *a* content at all the time intervals (almost 3 times higher at T15), nevertheless, between the As exposed concentrations significant differences were noticed from T9 until T21.

The changes in algal cell density (Fig. 1b) were coherent with the Chl *a* for all treatments (control, As (11.25 µg/L) and As (22.5 µg/L) from T3 to T21). The cell density in control was higher from T6 until T21, increasing significantly from T6, T9, T12 until T15 reaching 27.6×10^6 cells/mL and thereafter decreasing in the lysis phase at T21. The cell density of As (11.25 µg/L) increased significantly from T9 to T12 thereby decreasing at T21. Similarly, the cell density in As (22.5 µg/L) treatment increased significantly from T6, T9 to T12 and decreased at T21. However, in between the treatments, significant differences were observed between control and As exposures at all the phases from T9 until T21. In between the two As concentrations, algal cell density differed significantly from T12 until T21.

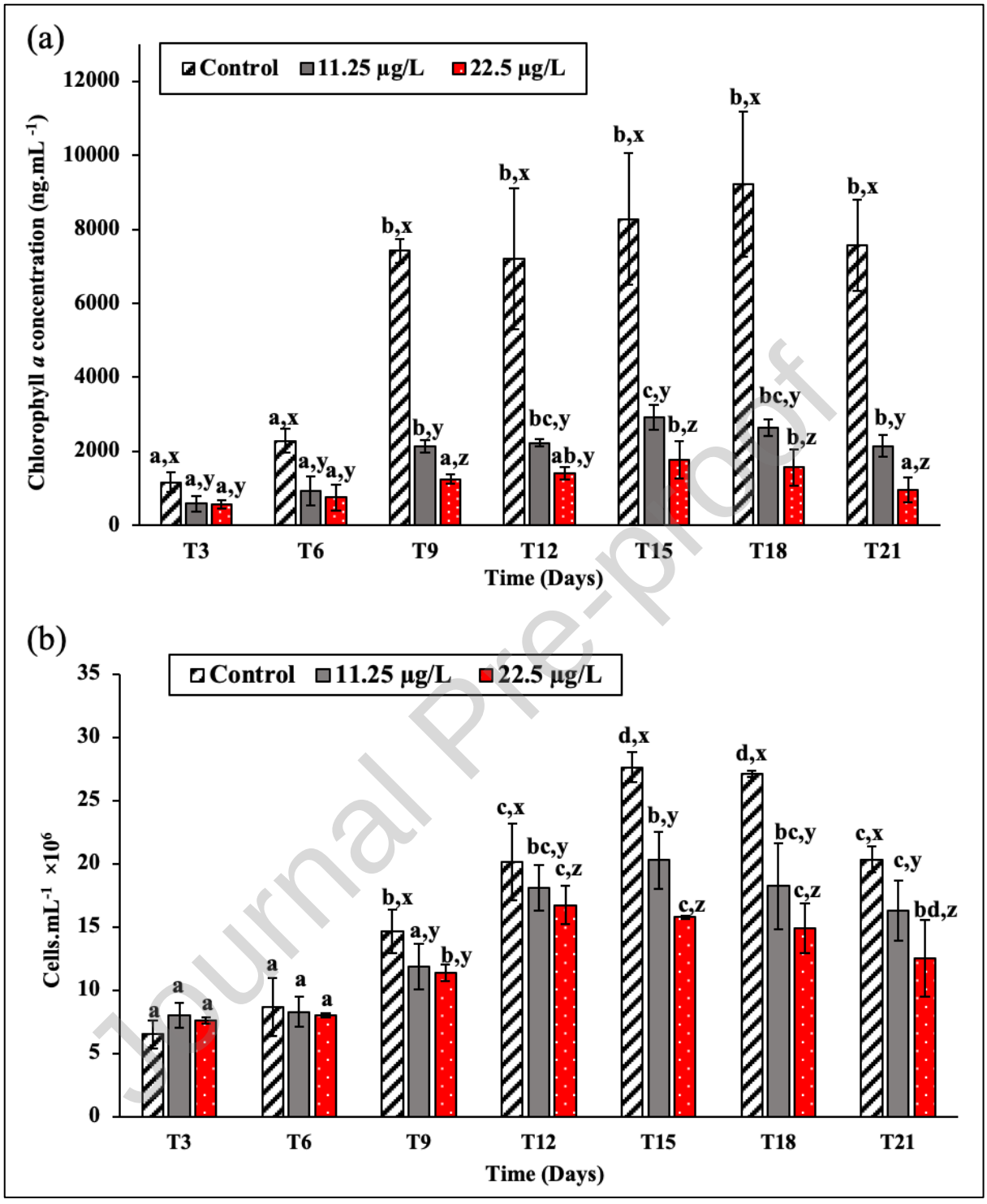

Fig. 1a. Chlorophyll *a* content in *D. lutheri* for all the treatments from T3 to T21 of the algal growth phase. Alphabets a, b, c shows significant differences between incubation times; x, y, z shows significant differences between treatments, at $p < 0.05$. Error bar denotes standard deviation between the replicates in each treatment (n = 3). Fig.1b. The growth curve of *D. lutheri* showing cell counts every three days for control, As (11.25 µg/L) and As (22.5 µg/L).

Alphabets a, b, c, d shows significant differences between incubation times; x, y, z shows significant differences between treatments, at $p < 0.05$. Error bar denotes standard deviation between the replicates in each treatment (n = 3).

3.2 Physiological state of *D. lutheri*

The maximum quantum yield F_v/F_m shows a very different temporal pattern from previous parameters for control and arsenic-contaminated conditions (As (11.25 µg/L) and As (22.5 µg/L)) at the same measurement frequency (from T3 to T21). The F_v/F_m values for the control displayed higher values than As conditions all along the incubation period although being significantly higher (ANOVA, $p < 0.05$) after T12 until the lysis phase (T21). For control treatment no significant differences were observed between the different incubation times, i.e. throughout the growth curve. The treatment As (22.5 µg/L) showed lower values of F_v/F_m than As (11.25 µg/L) at all the measured intervals however differences were not statistically significant. The F_v/F_m values for As (11.25 µg/L) and (22.5 µg/L) decreased significantly over the growth curve; from T3 to T6 and further to T15 thereafter getting almost stable until T21. In general, there was an overall change in F_v/F_m values over time: at T3, the F_v/F_m values were greater than 0.35 for the 3 experimental conditions and they became less than 0.2 for the As exposed treatments from time T15. For control, the values decreased at the beginning but always remained above 0.3. This means that the physiological state of the As contaminated cells deteriorated more than that of control. Low F_v/F_m values ranging between 0.3 and 0.4, that is below the theoretical threshold of 0.7 corresponding to a very good physiological state, are extremely common for microalgae cultures of very high concentrations: for example, the recent studies of Gan et al., 2019 and Papry et al., 2021 reported similar observations on lead

and arsenic toxicity respectively. These F_v/F_m values are mainly explained by the light and nutrient limitation conditions of very dense cultures.

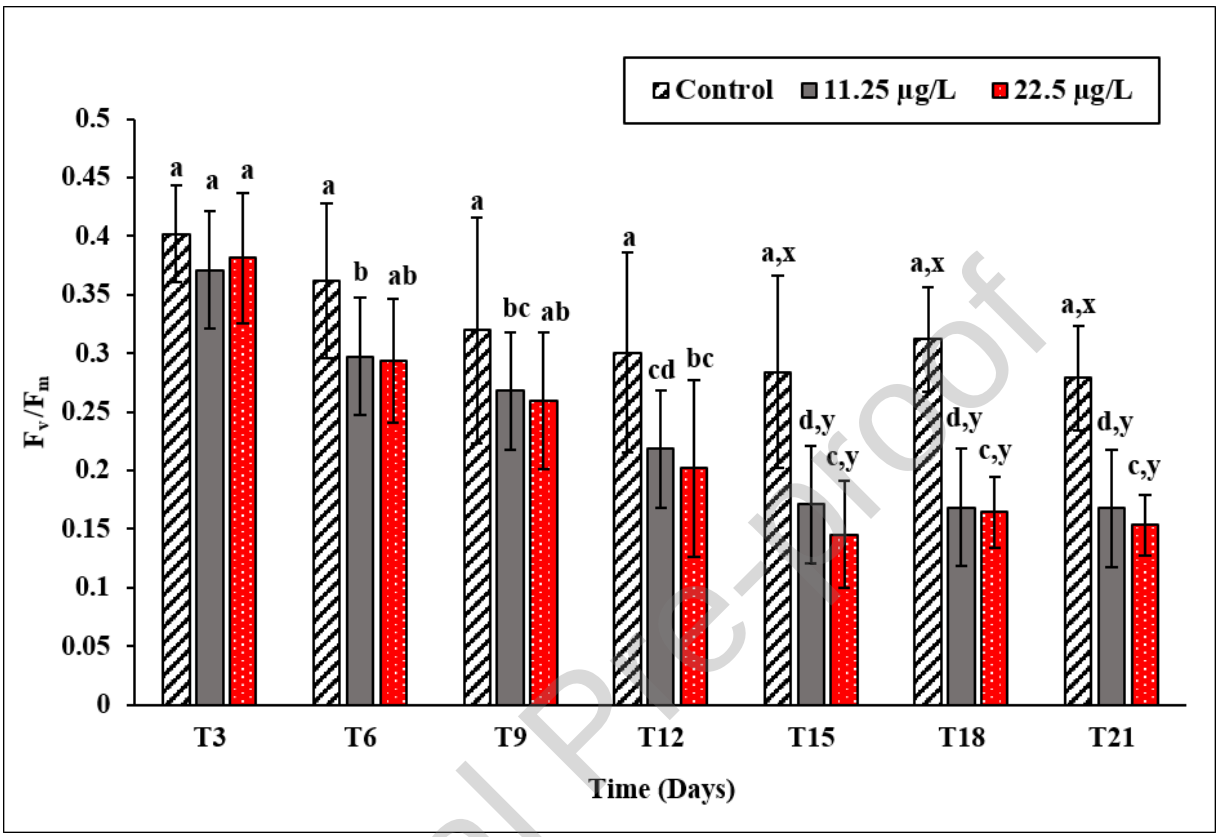

Fig. 2. Maximum quantum yield F_v/F_m values for control, As (11.25 µg/L) and As (22.5 µg/L) treatments from T3 until T21 of the experiment. Alphabets a, b, c, d shows significant differences between incubation times; x, y shows significant differences between treatments, at $p < 0.05$. Error bar denotes standard deviation between the replicates in each treatment (n = 3).

3.3 Photo-physiological properties

Of all the parameters studied that describe photosynthetic processes by variable fluorescence (FRRf technique), we present below the most relevant ones given our initial objectives. This is why parameters describing the photosynthesis-energy relationships in absolute units [as the absolute light utilization efficiency (α_{II})], were not selected for a detailed discussion, but is

displayed in the Supplementary Material (Section 2.1S, Fig. 2S) and will be cited when necessary. The parameter 1/Tau' is also attached in the supplementary material in the section 2.4S (Fig. 4S).

3.3.1 Light absorption properties

Firstly, the functional light absorption of PSII [the Sigma (σ_{PSII}) parameter] was always the lowest for the control condition and the highest for As (22.5 µg/L) treatment from T3 to T21, showing significant differences between the two groups ($p < 0.05$) (Fig. 3a). σ_{PSII} showed for both the As exposed treatments a strong and significant increase between T6 and T9 remaining constant until the end of the growth curve (T21). On the contrary for the control condition, σ_{PSII} did not change significantly with time (as for F_v/F_m), showing a slight increase at T15 and T18.

Secondly, the optical absorption cross section parameter (a_{LHII}) (Fig. 3b) of the light harvesting pigments of PSII had a slightly different temporal variation pattern of $\sigma_{PSII.}$ The comparison between the three exposures showed that As (22.5 µg/L) treatment had the highest value of a_{LHII} at every sampling time. The control showed the lowest values differing significantly from the As exposed treatments from T12 until T21. However, a_{LHII} showed, unlike Sigma (σ_{PSII}), a significant increase in control treatment from T3 to T9 and at T21. In addition, As (22.5 µg/L) showed significantly higher a_{LHII} values than As (11.25 µg/L), whereas such significant differences between the low (11.25 µg/L) and high (22.5 µg/L) concentration of As treatments were not observed for the two previous parameters, F_v/F_m and Sigma (σ_{PSII}). Note that it is this increase in light absorption through a_{LHII} that induces an increase in the absolute light utilization efficiency (Fig. 2S), given the model described in equation 3.

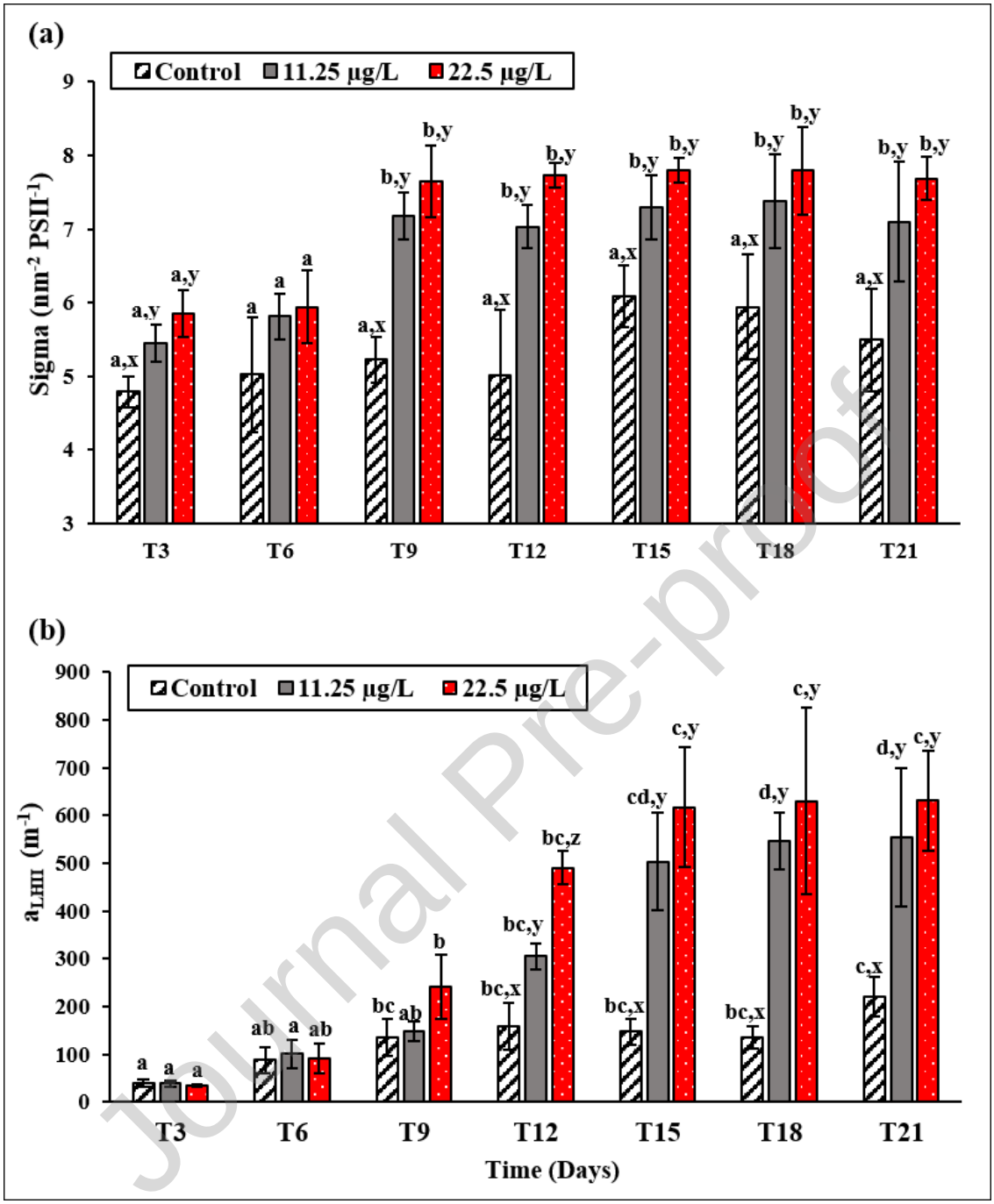

Fig. 3a. Sigma (in nm^2 $PSII^{-1}$) values for control, As (11.25 µg/L) and As (22.5 µg/L) treatment from T3 until T21. **Fig. 3b.** a_{LHII} (in m^{-1}) values of control, As (11.25 µg/L) and As (22.5 µg/L) treatment from T3 until T21. Alphabets a, b, c shows significant differences between incubation times; x, y, z shows significant differences between treatments, at $p < 0.05$. Error bar denotes standard deviation between the replicates in each treatment (n = 3).

3.3.2 NPQ-NSV

Fig. 4 shows the relationship between the NPQ-NSV and the de-epoxidation ratio (DR) in control, As (11.25 µg/L) and As (22.5 µg/L), at all the measured time intervals. In the plot area, the smallest icon for each individual treatment denotes the values for T3, thereby increasing gradually with the time of exposure, with largest icons denoting T21. More precisely, the figure 6 shows the positive correlation between the NPQ-NSV and the de-epoxidation ratio (DR), when values of As (11.25 µg/L) and As (22.5 µg/L) were combined, showing an R^2 value of 0.842 and a p-value of < 0.01. The relationship between NPQ-NSV and DR in the control treatment showed a totally different slope and range of variation, which could be related to different cell needs in control conditions, in terms of energy photo-regulation, compared to cells under arsenic which show strong increases in light absorption. Such positive and highly significant correlation illustrates the efficiency of energy dissipation by photoprotective pigments in As conditions and control. No significant differences were observed in between the two As concentrations.

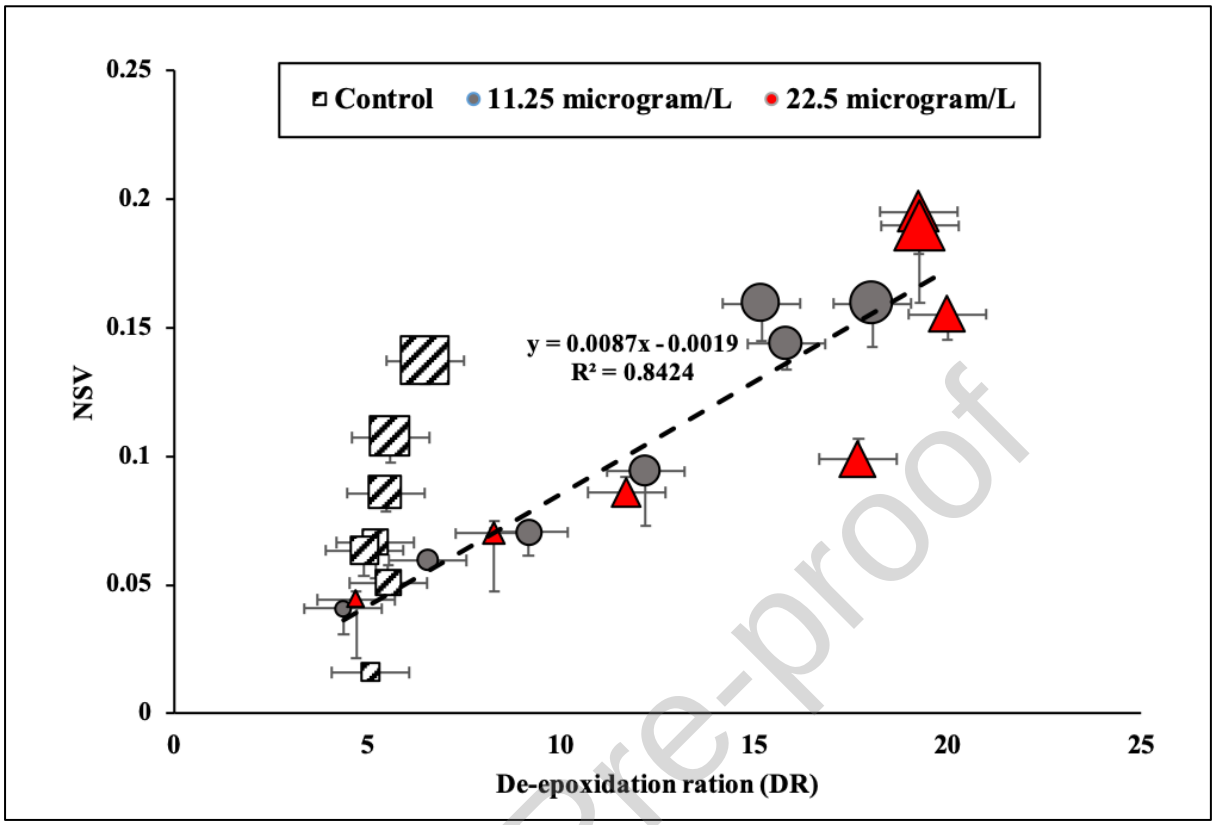

Fig. 4. Linear relationship between the values of NPQ-NSV and de-epoxidation ratio (DR) As (11.25 µg/L) and As (22.5 µg/L) treatment from T3 (smallest icon) until T21 (largest icon) for each individual treatment. The p value was calculated by comparing the treatments with Pearson's correlation.

3.4 Bioaccumulation of trace metals by *D. lutheri*

Fig. 5 shows the concentration of total As and Iron (Fe) bioaccumulated by *D. lutheri* in control and the arsenic exposed treatments. The figure shows a scatter plot to highlight the relationship between the As and Fe accumulation by *D. lutheri*, where the combined trend of the arsenic exposed treatments [As (11.25 µg/L) and As (22.5 µg/L)] shows a linear positive correlation with a p value of <0.01 (linear R, Pearson). On the contrary, the control shows no such positive correlation between the concentration of As and Fe when bioaccumulated by the microalgae. The figure displaying the concentration of total As bioaccumulated by *D. lutheri* is added in the supplementary file (Fig. 3S).

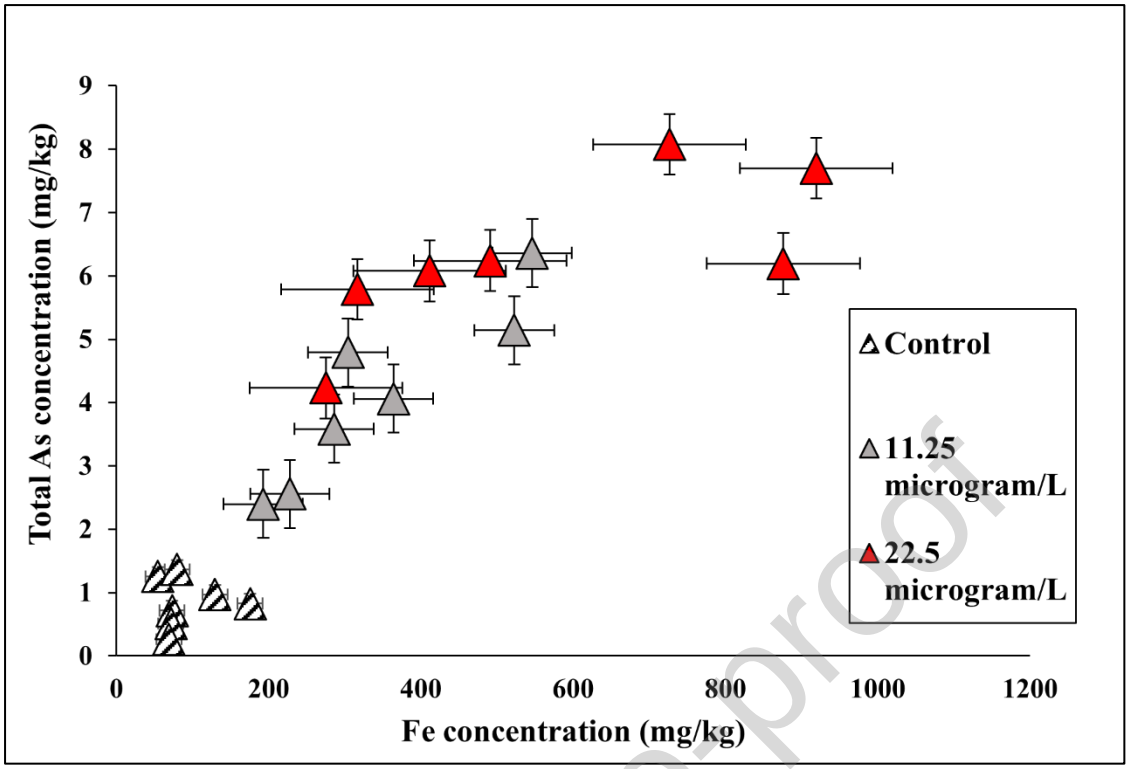

Fig. 5. Linear relationship between the bioaccumulation of total As and Iron (Fe) in control, As (11.25 µg/L) and As (22.5 µg/L). The p value was calculated by comparing the arsenic exposed treatments with Pearson's correlation (n = 3).

4. Discussion

4.1 Toxicity of Arsenic to *D. lutheri*

The growth curve of *D. lutheri* in this study, showed a clear and strong slowdown in arsenic exposed cells, consistently explained from all the parameters measured, like the cell density, pigments and photo-physiology by variable fluorescence. The cell density of *D. lutheri* showed a significant difference from the control after 9 days of As exposure irrespective of the concentration. Non-essential trace metal exposures often caused a significant drop in cell density or growth rates at the post exponential phase of an algal growth indicating the failure to combat both the toxic chemicals and the declining amount of nutrients towards the end of the growth period (Navarrete et al., 2019 ; Huang et al., 2021 ; Das et al., 2022a). Huang et al., 2021 reported that the effect of As exposure on the cell growth was observed after 10

days irrespective of the concentration used in their study. Our study reports that *D. lutheri* could combat the effect of the stress from As exposure until the beginning of post exponential phase (T= 12) which is noted in studies that use environmentally realistic concentration of trace metals in their toxicological assays (Hussain et al., 2021; Huang et al., 2021; Das et al., 2022a). Such withstand to the harmful effects can cause a number of physiological changes in the photosynthetic machinery of microalgal cells that is trying to adapt to the added stress (arsenic stress, in this study) (Dao and Beardall, 2016a; Dao and Beardall, 2016b; Gan et al., 2019). These physiological changes analysed with the variable fluorescence were coherent with the biomass patterns (cell density) further indicating a directly proportional relation with the pigment concentrations (chl *a* and DR) evaluated in this study. For instance, the lower values of the maximum photosynthetic quantum yield F_v/F_m and the enhancement of the light absorption capacity (Sigma and a_{LHII}) and of the non-photochemical energy dissipation NPQ-NSV were here well in line with the pigment concentration like the lower chl *a* and the higher ratio of de-epoxidation (photo-protective pigments) analysed for the arsenic exposed treatments. Basically, the exposure to arsenic generated strong physiological responses due to numerous disturbances caused by arsenic inside the algal cells. The control that showed an increase in biomass did not show a joint increase in light absorption that could be a response to self-shading. The strong increases of Sigma and much more of aLHII were therefore specific to the conditions of intoxication by As. Previous studies have discussed the phenomena of the gradual binding of trace metals to sulfhydryl groups that makes the microalgae lose its absorptive potential to intake nutrients that are necessary for a proper metabolic functioning (Hu and Zhou, 2010; Chia et al., 2015; Hussain et al., 2021; Das et al., 2022a) . In addition, trace metals can substitute the magnesium binding and create loose ligands that affect majorly the synthesis of photosynthetic pigments as a result generating lower biomass (Dao and Beardall, 2016b; Dao and Beardall, 2016a; Grajek et al., 2020; Chu

et al., 2022; Zong et al., 2021). Arsenic, being non-essential and highly toxic was reported to disrupt cell membranes primarily and thereby affect uptake of nutrients by attaching themselves to the thiol groups and replacing phosphate ions which in turn impairs the antioxidant defense mechanisms (Chandrakar et al., 2018; Cai et al., 2021) and the energy flux of the photosynthetic machinery (Zhang et al., 2021; Samanta et al., 2022).

As a whole, combining all the results of pigment profile, growth and the physiological variables, some photosynthetic parameters are noted to be elevated for the arsenic contaminated cells. On contrary, biomass and pigment concentrations were significantly lowered compared to control. This phenomenon was explained by Jacob-Lopes et al., 2017, as an inhibition of enzymatic activity like RuBisCO (ribulose-1,5-biphosphate carboxylase oxygenase, EC: EC 4.1.1.39) which is a key enzyme responsible for the carbon fixation in biomass. We report that the biomass in the arsenic exposed treatment in this study was significantly hindered due to the lack of carbon fixation inside the microalgal cells that presumably caused an increase in light absorption, but without altering the main photosynthetic process, which is the electron flux between the two photosystems, as shown by the strong absolute light utilization efficiency values (Fig. 2S). Indeed, the 1/Tau'(Fig 4S, supplementary file) parameter indicating the rate of re-opening of a closed RCII with an empty plastoquinone B site showed significant higher values between control and As-exposed cultures. According to Dhir et al., 2011, a wide range of trace metals acutely decreased the capacity of the fixation of carbon in *Salvinia natans*. The authors further discussed that the major cause of a lower biomass was the disruption of the enzymatic activity of RuBisCO usually caused when trace metals replace important elements like magnesium and phosphate ions responsible for various biochemical reactions (Dhir et al., 2011; DalCorso, 2012; Papry et al., 2021; Papry et al., 2022). Previous literatures further discussed on the role of trace metals to dissociate varied units (by size) of RuBisCO which

results in the blockage and/or an inhibition of it (Galmés et al., 2013; Portis, 2003) . The replacement of essential nutrients (like Magnesium, Phosphate) and binding of trace metals often diminishes the synthesis of photosynthetic pigments which further decreases the activity of the RuBisCO enzyme (Galmés et al., 2013; Pietrini et al., 2003). The results of our study reports that the main alteration caused in As exposed algal cells can be the incapacity for the assimilation of carbon dioxide due to the attachment of the trace metals, which might have inhibited the essential enzymatic activity like that of RuBisCO, retarding cell growth and biomass (Mamun et al., 2019b; Mamun et al., 2019a; Chen et al., 2021). Furthermore, the increasing light absorption along with the inability in carbon fixation over the course of the exposure time, generated excessive energy flux to be managed by the cells. As a result, this energy was dissipated as heat (NPQ-NSV) given the fact that the cells were unable to utilize it successfully due to the binding of trace metals (Lacour et al., 2018; Schuback et al., 2021b; Hoang et al., 2020). The increase in electron flux in the photosynthetic chain with regard to the absolute light utilization efficiency without positive effect on growth, can be explained by alternative electron flow as the cyclic electron flow around photosystem I (a well-known process that cannot be studied by variable fluorescence) that could increase under stress conditions for cells (Cardol et al., 2011) parallel to the NPQ -NSV (energy dissipation). This study reports the strong relationship of the variable fluorescence indicator of higher energy dissipation (NPQ-NSV) with the reversible process allying the photoprotective pigments diadinoxanthin and diatoxanthin often known as the de-epoxidation ratio (DR) from the arsenic exposed treatments with increasing time of exposure (Bertrand et al., 2001; Ji et al., 2018; Zsiros et al., 2020; Das et al., 2022a).

4.2 Rapid indicators of metal toxicity

Previous literatures reported the efficiency of using FRRf technique in providing valuable parameters that affects the PSII machinery in a range of microalgal species when exposed to

various contaminants like Copper (Cu), Mercury (Hg) and organic contaminants like herbicides, fungicides (Dao and Beardall, 2016a; Dao and Beardall, 2016b; Gan et al., 2019; Beaulieu et al., 2020; Chen et al., 2021). Our study supports the fact that FRRf technique is highly effective in providing physiological parameters, rapidly, that reflects the alterations caused from As stress. Papry et al., 2021 also worked with FRRf on the issue of arsenic toxicity for different experimental conditions, only with F_v/F_m parameter without characterizing the effects of As on the modifications of energy photo-regulation in the cell (NPQ-NSV, 1/Tau'). The maximum quantum efficiency F_v/F_m is often referred as a key parameter due to its pertinence in reflecting the biological functioning inside the reaction centers of the PSII (Kim Tiam et al., 2015; Mamun et al., 2019a; Mamun et al., 2019b; Chen et al., 2021). Our results correspond to higher values of F_v/F_m in the uncontaminated and healthy cells of the control treatment differing significantly from the As exposed algal cells (Moore et al., 2006; Moore et al., 2007; Zhu et al., 2019; Wang et al., 2020; Bhagooli et al., 2021). In spite of its great significance, previous studies to a large extent could not optimally use F_v/F_m as a suitable indicator to sublethal toxic exposures and denoted it as a species-specific indicator, (Dao and Beardall, 2016a; Dao and Beardall, 2016b; Mamun et al., 2019a; Mamun et al., 2019a; Chen et al., 2021) which is often dependent on available nutrient concentrations (Napoléon et al., 2013). Our study supports this observation and proposes some photo-physiological parameters like the a_{LHII}, Sigma and NPQ-NSV or 1/Tau exemplifying higher sensitivity to As toxicity with respect to the time of exposure and concentration. Among them, the optical absorption cross section of the light-harvesting pigments (a_{LHII} in m^{-1}) increased progressively at T9 for the higher As concentration, significantly differing between each treatment at T12, whereas Sigma (functional absorption cross section) increased at T9 and thereafter remained constant exhibiting no such significant differences between the As exposed groups. Dao and Beardall, 2016a , identified that both

the optical absorption and the functional absorption cross section significantly increased when two freshwater microalgae as *Chlorella* sp and *Scenedesmus* sp was exposed to Pb. In agreement to the above report, our study further suggests that a_{LHII} is an attractive parameter to rapidly detect As toxicity and can be used in signaling trace metal stress by environmental risk assessors especially in contaminated groundwater that are often consumed by local residents (Hussain et al., 2021).

The suitability of a small-sized antenna in light transmissivity and reduction of excessive dispersion of energy to produce higher biomass is well known in the studies concerning photosynthetic machineries (Polle et al., 2002; Dao and Beardall, 2016a; Dao and Beardall, 2016b; Bhagooli et al., 2021; Beaulieu et al., 2020). In this context, the elevation of both the functional and optical absorption cross section, NPQ-NSV and 1/Tau in arsenic exposed algal cells illustrate an abnormal physiological reaction and photo-regulation processes with regard to conventional light conditions and the temperature of the culture conditions. Such indications of toxicity from photo-physiological parameters are rarely investigated and can be specified by the variable fluorescence technique deemed as being a non-destructive and a rapid method (Gan et al., 2019; Chen et al., 2021). Previous studies also suggested that during state transitions, relocation of the light harvesting complex (LHC) between the two photosystems can be distorted when toxic chemical substances affect the phosphorylation of LHC, which is necessary to modulate the energy involved in the photochemical reactions (Falkowski and Raven, 2013; Ünlü et al., 2014; Dao and Beardall, 2016a). This omission of phosphorylation of LHC due to the exposure to trace metals can extend the absorption cross section, which is reported in literature and our results are in accordance with this finding (Belatik et al., 2013; Falkowski and Raven, 2013). Along with the Sigma and a_{LHII}, we also propose NPQ-NSV as a suitable indicator to arsenic stress related to the high energy dissipation as a function of producing higher photoprotective pigments. It should also be

noted that conventional photosynthetic parameters describing the Photosynthesis-Energy relationships are less effective in characterizing the toxicity of arsenic exposures (in Supplementary materials). It is the so-called primary parameters (Schuback et al., 2021a), such as NPQ-NSV and also 1/Tau that are more effective for this. This inability was well indicated by the non-photochemical quenching (NSV) parameter that was consistent with the respective photoprotective pigment profile. Hence, the benign, non-polluting and rapid protocols of FRRf used to detect toxicity of hazardous trace metals like arsenic can be promoted in ecotoxicological assays in which the use of usual laboratory methods that are tedious, time taking and often destructive are mostly in practice and is widespread.

4.3 Bioaccumulation of Arsenic

The adsorption of As by microalgae has been demonstrated as a complex process involving bioaccumulation, biotransformation of inorganic As (As^{V} and As^{III}) to organic forms (methylated, methylarsenic), along with cycling of As species in the environment (Kalla and Khan, 2016; Papry et al., 2022). Previous literature also mentioned the possibility of bioremediation of As by using microalgae given their role and efficiency in the mechanism of biotransformation (Mamun et al., 2019a; Mamun et al., 2019b; Das et al., 2022a; (Papry et al., 2022). Our study reports the highest total As concentration bioaccumulated by *D. lutheri* from the As (22.5 µg/L) treatment at day 12 (post-exponential phase) of the algal growth curve. In addition, the post exponential phase also marked the significant declination in cell density, chl *a* content and maximum quantum efficiency (Fv/Fm) in As exposed *D. lutheri* cells. The highest concentration of As accumulation by *D. lutheri* and the significant differences between the low and the high concentration of As treatment in optical absorption cross section at day 12 is also noteworthy. Previous studies on lead (Pb) toxicity by Dao and Beardall, 2016b and later by Gan et al., 2019 reported that a series of photosynthetic

parameters were inhibited on the basis of the concentration of Pb and the time of incubation. According to Mamun et al., 2019a and Mamun et al., 2019b the presence of Fe plaque on the surface on the algal cells had an effect on the bioaccumulation of As. These studies further reported that Fe plays an important role showing a positive correlation in forming a complex with trace elements and nutrients prevailing in the environment (Mamun et al., 2019a; (Mamun et al., 2019b); (Carneiro et al., 2022); (Hasegawa et al., 2022). In this study we had a similar observation of a strong positive correlation between Fe and As concentration bioaccumulated by *D. lutheri*. In our previous study a co-exposure of a cocktail of trace metals with As also showed the altered bioconcentration factor and bioaccumulation compared to the single exposure of As (Das et al., 2022) . Hence, uptake of As by microalgae depends on varied factors, like that of the presence of other metals and nutrients and a detailed study on the mechanism of biotransformation and/or speciation of As on *D. lutheri* is yet unsettled, which can be considered in the future given the importance of this microalgal species in commercial grounds.

5. Conclusion

This study shows the effect of As contamination on the physiology, pigment concentrations and cell density of the algal species *D. lutheri* throughout the algal growth curve. The cell density, chl *a* concentration decreased significantly in As exposed cells from day 9 until the lysis phase day 21 when compared to the control. The maximum quantum efficiency (F_v/F_m) showed coherence with the growth parameters whereas the photo-physiological parameters like the functional [Sigma (σ_{PSII})] and the optical (a_{LHII}) absorption cross section of *D. lutheri* cells enhanced when exposed to Arsenic in both the low (11.25 µg/L) and high concentration (22.5 µg/L). The inability to produce biomass, yet a high light absorption presumably led to higher dissipation of heat (NPQ-NSV) in the As exposed algal cells. In addition, the FRRf

parameter NPQ-NSV showed a strong correlation with the HPLC obtained de-epoxidation ratio involving the photoprotective pigments only in the As exposed treatments differing significantly from the control. Such indicators of As toxicity analysed with rapidity and precision, involving non-destructive processes using microalgae are infrequent, but are priorities in the area of environmental health assessments. Our study proffers such indicators and suggests that the photo-physiological factors of *D. lutheri* exemplified better proxies for signalling the environmentally realistic concentrations of As than conventional parameters. A strong correlation between Fe and As bioaccumulation was observed in *D. lutheri* which is the characteristic of Fe in sequestration of other trace metals. Hence in this study both variable fluorescence and HPLC parameters showed coherence further justifying the accuracy in implementing these novel indicators. Nonetheless, the use of environmentally realistic concentration of As in our study helps not to restrict the proposed indicators to only laboratory-based assays.

Acknowledgement

We are thankful to the project Valgorize (Interreg 2 Seas programme) co-funded by the European Regional Development Fund under the subsidy contract No ValgOrize 2S05017 for providing the necessary fellowship to perform this study. Our earnest gratitude to the past and present members of our laboratory for maintaining the mass-cultures of planktons for years. This work has been supported by the European Union (ERDF), the French State, the French Region Hauts-de-France and Ifremer, in the framework of the project CPER MARCO 2015-2021. We thank the Communaut´e d'Agglom´eration du Boulonnais (CAB) for the implementation of a copepod-rearing pilot project (agreement 'HALIOCAP' Universit´e de Lille-CAB) and the Chevreul Institute Platform (U-Lille/CNRS) for the ICP-AES and ICP-MS measurements. This work is a contribution to the International Associated Laboratory

between Université de Lille and National Taiwan Ocean University (IAL MULTIFAQUA).

This paper is a contribution to the project CPER IDEAL for their assistance.

References

Aardema, H.M., Rijkeboer, M., Lefebvre, A., Veen, A., Kromkamp, J.C., 2019. High-resolution underway measurements of phytoplankton photosynthesis and abundance as an innovative addition to water quality monitoring programs. Ocean Sci. 15, 1267–1285. https://doi.org/10.5194/os-15-1267-2019

Aboal, J.R., Pacín, C., García-Seoane, R., Varela, Z., González, A.G., Fernández, J.A., 2022. Global decrease in heavy metal concentrations in brown algae in the last 90 years. J. Hazard. Mater. 130511. https://doi.org/10.1016/j.jhazmat.2022.130511

Ahmed, F., Zhou, W., Schenk, P.M., 2015. Pavlova lutheri is a high-level producer of phytosterols. Algal Res. 10, 210–217. https://doi.org/10.1016/j.algal.2015.05.013

Anawar, H.M., Rengel, Z., Damon, P., Tibbett, M., 2018. Arsenic-phosphorus interactions in the soil-plant-microbe system: Dynamics of uptake, suppression and toxicity to plants. Environ. Pollut. 233, 1003–1012. https://doi.org/10.1016/j.envpol.2017.09.098

Arias, A.H., Souissi, A., Glippa, O., Roussin, M., Dumoulin, D., Net, S., Ouddane, B., Souissi, S., 2017. Removal and Biodegradation of Phenanthrene, Fluoranthene and Pyrene by the Marine Algae Rhodomonas baltica Enriched from North Atlantic Coasts. Bull. Environ. Contam. Toxicol. 98, 392–399. https://doi.org/10.1007/s00128-016-1967-4

Arsalane, W., Rousseau, B., Duval, J.-C., 1994. Influence of the Pool Size of the Xanthophyll Cycle on the Effects of Light Stress in a Diatom: Competition Between Photoproteci'ion and Photoinhibition. Photochem. Photobiol. 60, 237–243. https://doi.org/10.1111/j.1751-1097.1994.tb05097.x

Banks, J.M., 2018. Chlorophyll fluorescence as a tool to identify drought stress in Acer genotypes. Environ. Exp. Bot. 155, 118–127. https://doi.org/10.1016/j.envexpbot.2018.06.022

Beaulieu, M., Cabana, H., Huot, Y., 2020. Adverse effects of atrazine, DCMU and metolachlor on phytoplankton cultures and communities at environmentally relevant concentrations using Fast Repetition Rate Fluorescence. Sci. Total Environ. 712, 136239. https://doi.org/10.1016/j.scitotenv.2019.136239

Belatik, A., Hotchandani, S., Carpentier, R., 2013. Inhibition of the Water Oxidizing Complex of Photosystem II and the Reoxidation of the Quinone Acceptor QA− by Pb2+. PLOS ONE 8, e68142. https://doi.org/10.1371/journal.pone.0068142

Bertrand, M., Schoefs, B., Siffel, P., Rohacek, K., Molnar, I., 2001. Cadmium inhibits epoxidation of diatoxanthin to diadinoxanthin in the xanthophyll cycle of the marine diatom Phaeodactylum tricornutum. FEBS Lett. 508, 153–156. https://doi.org/10.1016/S0014-5793(01)03050-2

Bhagooli, R., Mattan-Moorgawa, S., Kaullysing, D., Louis, Y.D., Gopeechund, A., Ramah, S., Soondur, M., Pilly, S.S., Beesoo, R., Wijayanti, D.P., Bachok, Z.B., Monrás, V.C., Casareto, B.E., Suzuki, Y., Baker, A.C., 2021. Chlorophyll fluorescence – A tool to assess photosynthetic performance and stress photophysiology in symbiotic marine invertebrates and seaplants. Mar. Pollut. Bull. 165, 112059. https://doi.org/10.1016/j.marpolbul.2021.112059

Brunet, C., Chandrasekaran, R., Barra, L., Giovagnetti, V., Corato, F., Ruban, A.V., 2014. Spectral Radiation Dependent Photoprotective Mechanism in the Diatom Pseudo-nitzschia multistriata. PLoS ONE 9, e87015. https://doi.org/10.1371/journal.pone.0087015

Cai, W., Chen, T., Lei, M., Wan, X., 2021. Effective strategy to recycle arsenic-accumulated biomass of Pteris vittata with high benefits. Sci. Total Environ. 756, 143890. https://doi.org/10.1016/j.scitotenv.2020.143890

Cardol, P., Forti, G., Finazzi, G., 2011. Regulation of electron transport in microalgae. Biochim. Biophys. Acta BBA - Bioenerg. 1807, 912–918. https://doi.org/10.1016/j.bbabio.2010.12.004

Carneiro, M.A., Pintor, A.M.A., Boaventura, R.A.R., Botelho, C.M.S., 2022. Efficient removal of arsenic from aqueous solution by continuous adsorption onto iron-coated cork granulates. J. Hazard. Mater. 432, 128657. https://doi.org/10.1016/j.jhazmat.2022.128657

Carvalho, A.P., Monteiro, C.M., Malcata, F.X., 2009. Simultaneous effect of irradiance and temperature on biochemical composition of the microalga Pavlova lutheri. J. Appl. Phycol. 21, 543–552. https://doi.org/10.1007/s10811-009-9415-z

Chandrakar, V., Dubey, A., Keshavkant, S., 2018. Modulation of arsenic-induced oxidative stress and protein metabolism by diphenyleneiodonium, 24-epibrassinolide and proline in Glycine max L. Acta Bot. Croat. 77, 51–61. https://doi.org/10.2478/botcro-2018-0004

Chen, M., Yin, G., Zhao, N., Gan, T., Feng, C., Gu, M., Qi, P., Ding, Z., 2021. Rapid and Sensitive Detection of Water Toxicity Based on Photosynthetic Inhibition Effect. Toxics 9, 321. https://doi.org/10.3390/toxics9120321

Chia, M.A., Chimdirim, P.K., Japhet, W.S., 2015. Lead induced antioxidant response and phenotypic plasticity of Scenedesmus quadricauda (Turp.) de Brébisson under different nitrogen concentrations. J. Appl. Phycol. 27, 293–302. https://doi.org/10.1007/s10811-014-0312-8

Chiellini, C., Guglielminetti, L., Pistelli, L., Ciurli, A., 2020. Screening of trace metal elements for pollution tolerance of freshwater and marine microalgal strains: Overview and perspectives. Algal Res. 45, 101751. https://doi.org/10.1016/j.algal.2019.101751

Chu, S., Feng, X., Liu, C., Wu, H., Liu, X., 2022. Advances in Chelating Resins for Adsorption of Heavy Metal Ions. Ind. Eng. Chem. Res. 61, 11309–11328. https://doi.org/10.1021/acs.iecr.2c01353

Cima, F., Craig, P.J., Harrington, C.F., 2003. Organotin Compounds in the Environment, in: Craig, P.J. (Ed.), Organometallic Compounds in the Environment. John Wiley & Sons, Ltd, Chichester, UK, pp. 101–149. https://doi.org/10.1002/0470867868.ch3

Costa, G.B., Ramlov, F., Koerich, G., Navarro, B.B., Cabral, D., Rodrigues, E.R.O., Ramos, B., Fadigas, S.D., Rörig, L.R., Maraschin, M., Horta, P.A., 2019. The effects of mining tailings in the physiology of benthic algae: Understanding the relation between mud's inductive acidification and the heavy metal's toxicity. Environ. Exp. Bot. 167, 103818. https://doi.org/10.1016/j.envexpbot.2019.103818

DalCorso, G., 2012. Heavy Metal Toxicity in Plants, in: Furini, A. (Ed.), Plants and Heavy Metals, SpringerBriefs in Molecular Science. Springer Netherlands, Dordrecht, pp. 1–25. https://doi.org/10.1007/978-94-007-4441-7_1

Dao, L.H.T., Beardall, J., 2016a. Effects of lead on growth, photosynthetic characteristics and production of reactive oxygen species of two freshwater green algae. Chemosphere 147, 420–429. https://doi.org/10.1016/j.chemosphere.2015.12.117

Dao, L.H.T., Beardall, J., 2016b. Effects of lead on two green microalgae Chlorella and Scenedesmus: photosystem II activity and heterogeneity. Algal Res. 16, 150–159. https://doi.org/10.1016/j.algal.2016.03.006

Das, S., Aria, A., Cheng, J.-O., Souissi, S., Hwang, J.-S., Ko, F.-C., 2020a. Occurrence and distribution of anthropogenic persistent organic pollutants in coastal sediments and mud shrimps from the wetland of central Taiwan. PLOS ONE 15, e0227367. https://doi.org/10.1371/journal.pone.0227367

Das, S., Gevaert, F., Ouddane, B., Duong, G., Souissi, S., 2022. Single toxicity of arsenic and combined trace metal exposure to a microalga of ecological and commercial interest: Diacronema lutheri. Chemosphere 291, 132949. https://doi.org/10.1016/j.chemosphere.2021.132949

Das, S., Ouddane, B., Hwang, J.-S., Souissi, S., 2020b. Intergenerational effects of resuspended sediment and trace metal mixtures on life cycle traits of a pelagic copepod. Environ. Pollut. 267, 115460. https://doi.org/10.1016/j.envpol.2020.115460

Das, S., Souissi, A., Ouddane, B., Hwang, J.-S., Souissi, S., 2023. Trace metals exposure in three different coastal compartments show specific morphological and reproductive traits across generations in a sentinel copepod. Sci. Total Environ. 859, 160378. https://doi.org/10.1016/j.scitotenv.2022.160378

Das, S., Tseng, L.-C., Chou, C., Wang, L., Souissi, S., Hwang, J.-S., 2019. Effects of cadmium exposure on antioxidant enzymes and histological changes in the mud shrimp Austinogebia edulis (Crustacea: Decapoda). Environ. Sci. Pollut. Res. 26, 7752–7762. https://doi.org/10.1007/s11356-018-04113-x

Das, S., Tseng, L.-C., Wang, L., Hwang, J.-S., 2017. Burrow characteristics of the mud shrimp Austinogebia edulis, an ecological engineer causing sediment modification of a tidal flat. PLOS ONE 12, e0187647. https://doi.org/10.1371/journal.pone.0187647

Dhir, B., Sharmila, P., Pardha Saradhi, P., Sharma, S., Kumar, R., Mehta, D., 2011. Heavy metal induced physiological alterations in Salvinia natans. Ecotoxicol. Environ. Saf. 74, 1678–1684. https://doi.org/10.1016/j.ecoenv.2011.05.009

Duncan, E.G., Maher, W.A., Foster, S.D., 2015. Contribution of Arsenic Species in Unicellular Algae to the Cycling of Arsenic in Marine Ecosystems. Environ. Sci. Technol. 49, 33–50. https://doi.org/10.1021/es504074z

Eilers, P.H.C., Peeters, J.C.H., 1988. A model for the relationship between light intensity and the rate of photosynthesis in phytoplankton. Ecol. Model. 42, 199–215. https://doi.org/10.1016/0304-3800(88)90057-9

Falkowski, P.G., Raven, J.A., 2013. Aquatic Photosynthesis: Second Edition. Princeton University Press.

Galmés, J., Aranjuelo, I., Medrano, H., Flexas, J., 2013. Variation in Rubisco content and activity under variable climatic factors. Photosynth. Res. 117, 73–90. https://doi.org/10.1007/s11120-013-9861-y

Gan, T., Zhao, N., Yin, G., Chen, M., Wang, X., Liu, J., Liu, W., 2019. Optimal chlorophyll fluorescence parameter selection for rapid and sensitive detection of lead toxicity to marine microalgae Nitzschia closterium based on chlorophyll fluorescence technology. J. Photochem. Photobiol. B 197, 111551. https://doi.org/10.1016/j.jphotobiol.2019.111551

Gnouma, A., Sadovskaya, I., Souissi, A., Sebai, K., Medhioub, A., Grard, T., Souissi, S., 2017. Changes in fatty acids profile, monosaccharide profile and protein content during batch growth of Isochrysis galbana (T.iso). Aquac. Res. 48, 4982–4990. https://doi.org/10.1111/are.13316

Grajek, H., Rydzyński, D., Piotrowicz-Cieślak, A., Herman, A., Maciejczyk, M., Wieczorek, Z., 2020. Cadmium ion-chlorophyll interaction – Examination of spectral properties and structure of the cadmium-chlorophyll complex and their relevance to photosynthesis inhibition. Chemosphere 261, 127434. https://doi.org/10.1016/j.chemosphere.2020.127434

Grotti, M., Lagomarsino, C., Goessler, W., Francesconi, K.A., Grotti, M., Lagomarsino, C., Goessler, W., Francesconi, K.A., 2010. Arsenic speciation in marine organisms from Antarctic coastal environments. Environ. Chem. 7, 207–214. https://doi.org/10.1071/EN09131

Hasegawa, H., Akhyar, O., Omori, Y., Kato, Y., Kosugi, C., Miki, O., Mashio, A.S., Papry, R.I., 2022. Role of Fe plaque on arsenic biotransformation by marine macroalgae. Sci. Total Environ. 802, 149776. https://doi.org/10.1016/j.scitotenv.2021.149776

Hasegawa, H., Sohrin, Y., Seki, K., Sato, M., Norisuye, K., Naito, K., Matsui, M., 2001. Biosynthesis and release of methylarsenic compounds during the growth of freshwater algae. Chemosphere 43, 265–272. https://doi.org/10.1016/S0045-6535(00)00137-5

Hoang, M.H., Kim, H.-S., Zulfugarov, I.S., Lee, C.-H., 2020. Down-Regulation of Zeaxanthin Epoxidation in Vascular Plant Leaves Under Normal and Photooxidative Stress Conditions. J. Plant Biol. 63, 331–336. https://doi.org/10.1007/s12374-020-09260-8

Hu, H., Zhou, Q., 2010. Regulation of inorganic carbon acquisition by nitrogen and phosphorus levels in the Nannochloropsis sp. World J. Microbiol. Biotechnol. 26, 957–961. https://doi.org/10.1007/s11274-009-0253-6

Huang, H., Xiao, X., Ghadouani, A., Wu, J., Nie, Z., Peng, C., Xu, X., Shi, J., 2015. Effects of Natural Flavonoids on Photosynthetic Activity and Cell Integrity in Microcystis aeruginosa. Toxins 7, 66–80. https://doi.org/10.3390/toxins7010066

Huang, Z., Chen, B., Zhang, J., Yang, C., Wang, J., Song, F., Li, S., 2021. Absorption and speciation of arsenic by microalgae under arsenic-copper Co-exposure. Ecotoxicol. Environ. Saf. 213, 112024. https://doi.org/10.1016/j.ecoenv.2021.112024

Hussain, M.M., Wang, J., Bibi, I., Shahid, M., Niazi, N.K., Iqbal, J., Mian, I.A., Shaheen, S.M., Bashir, S., Shah, N.S., Hina, K., Rinklebe, J., 2021. Arsenic speciation and biotransformation pathways in the aquatic ecosystem: The significance of algae. J. Hazard. Mater. 403, 124027. https://doi.org/10.1016/j.jhazmat.2020.124027

Jacob-Lopes, E., Zepka, L.Q., Queiroz, M.I., 2017. Chlorophyll. BoD – Books on Demand.

Ji, Y., Xie, X., Wang, G., 2018. Effects of the heavy metal cadmium on photosynthetic activity and the xanthophyll cycle in Phaeodactylum tricornutum. J. Oceanol. Limnol. 36, 2194–2201. https://doi.org/10.1007/s00343-019-7160-y

Kadiene, E.U., Meng, P.-J., Hwang, J.-S., Souissi, S., 2019. Acute and chronic toxicity of cadmium on the copepod Pseudodiaptomus annandalei: A life history traits approach. Chemosphere 233, 396–404.

Kalla, N., Khan, S., 2016. Effect of nitrogen, phosphorus concentrations, pH and salinity ranges on growth, biomass and lipid accumulation of Chlorella vulgaris. Int. J. Pharm. Sci. Res. IJPSR 7, 397–405.

Kim Tiam, S., Laviale, M., Feurtet-Mazel, A., Jan, G., Gonzalez, P., Mazzella, N., Morin, S., 2015. Herbicide toxicity on river biofilms assessed by pulse amplitude modulated (PAM) fluorometry. Aquat. Toxicol. 165, 160–171. https://doi.org/10.1016/j.aquatox.2015.05.001

Lacour, T., Larivière, J., Ferland, J., Bruyant, F., Lavaud, J., Babin, M., 2018. The Role of Sustained Photoprotective Non-photochemical Quenching in Low Temperature and High Light Acclimation in the Bloom-Forming Arctic Diatom Thalassiosira gravida. Front. Mar. Sci. 5.

Li, H., Cao, M., Zhang, Y., Liu, Z., 2021. Hydrothermal liquefaction accelerates the toxicity and solubility of arsenic in biowaste. J. Hazard. Mater. 418, 126341. https://doi.org/10.1016/j.jhazmat.2021.126341

Maher, D., Eyre, B.D., 2011. Benthic carbon metabolism in southeast Australian estuaries: habitat importance, driving forces, and application of artificial neural network models. Mar. Ecol. Prog. Ser. 439, 97–115. https://doi.org/10.3354/meps09336

Mamun, M.A.A., Omori, Y., Miki, O., Rahman, I.M.M., Mashio, A.S., Maki, T., Hasegawa, H., 2019a. Comparative biotransformation and detoxification potential of arsenic by three macroalgae species in seawater: Evidence from laboratory culture studies. Chemosphere 228, 117–127. https://doi.org/10.1016/j.chemosphere.2019.04.056

Mamun, M.A.A., Rahman, I.M.M., Datta, R.R., Kosugi, C., Mashio, A.S., Maki, T., Hasegawa, H., 2019b. Arsenic speciation and biotransformation by the marine macroalga Undaria pinnatifida in seawater: A culture medium study. Chemosphere 222, 705–713. https://doi.org/10.1016/j.chemosphere.2019.01.185

Martins, P.L.G., Marques, L.G., Colepicolo, P., 2015. Antioxidant enzymes are induced by phenol in the marine microalga Lingulodinium polyedrum. Ecotoxicol. Environ. Saf. 116, 84–89. https://doi.org/10.1016/j.ecoenv.2015.03.003

McKew, B.A., Davey, P., Finch, S.J., Hopkins, J., Lefebvre, S.C., Metodiev, M.V., Oxborough, K., Raines, C.A., Lawson, T., Geider, R.J., 2013. The trade-off between the light-harvesting and

photoprotective functions of fucoxanthin-chlorophyll proteins dominates light acclimation in Emiliania huxleyi (clone CCMP 1516). New Phytol. 200, 74–85. https://doi.org/10.1111/nph.12373

Moore, C.M., Seeyave, S., Hickman, A.E., Allen, J.T., Lucas, M.I., Planquette, H., Pollard, R.T., Poulton, A.J., 2007. Iron–light interactions during the CROZet natural iron bloom and EXport experiment (CROZEX) I: Phytoplankton growth and photophysiology. Deep Sea Res. Part II Top. Stud. Oceanogr., The Crozet Natural Iron Bloom and Export Experiment 54, 2045–2065. https://doi.org/10.1016/j.dsr2.2007.06.011

Moore, C.M., Suggett, D.J., Hickman, A.E., Kim, Y.-N., Tweddle, J.F., Sharples, J., Geider, R.J., Holligan, P.M., 2006. Phytoplankton photoacclimation and photoadaptation in response to environmental gradients in a shelf sea. Limnol. Oceanogr. 51, 936–949. https://doi.org/10.4319/lo.2006.51.2.0936

Morelli, E., Mascherpa, M.C., Scarano, G., 2005. Biosynthesis of Phytochelatins and Arsenic Accumulation in the Marine Microalga Phaeodactylum tricornutum in Response to Arsenate Exposure. Biometals 18, 587–593. https://doi.org/10.1007/s10534-005-2998-1

Napoléon, C., Fiant, L., Raimbault, V., Claquin, P., 2013. Study of dynamics of phytoplankton and photosynthetic parameters using opportunity ships in the western English Channel. J. Mar. Syst. 128, 146–158. https://doi.org/10.1016/j.jmarsys.2013.04.019

Navarrete, A., González, A., Gómez, M., Contreras, R.A., Díaz, P., Lobos, G., Brown, M.T., Sáez, C.A., Moenne, A., 2019. Copper excess detoxification is mediated by a coordinated and complementary induction of glutathione, phytochelatins and metallothioneins in the green seaweed Ulva compressa. Plant Physiol. Biochem. 135, 423–431. https://doi.org/10.1016/j.plaphy.2018.11.019

Ouddane, B., 1990. Comportement des éléments majeurs et mineurs dans un milieu soumis à des gradients physico-chimiques marqués : cas de l'estuaire de la Seine (These de doctorat). Lille 1.

Oxborough, K., Baker, N.R., 1997. Resolving chlorophyll a fluorescence images of photosynthetic efficiency into photochemical and non-photochemical components – calculation of qP and Fv-/Fm-; without measuring Fo-; Photosynth. Res. 54, 135–142. https://doi.org/10.1023/A:1005936823310

Oxborough, K., Moore, C.M., Suggett, D.J., Lawson, T., Chan, H.G., Geider, R.J., 2012. Direct estimation of functional PSII reaction center concentration and PSII electron flux on a volume basis: a new approach to the analysis of Fast Repetition Rate fluorometry (FRRf) data: Analysis of FRRf data: a new approach. Limnol. Oceanogr. Methods 10, 142–154. https://doi.org/10.4319/lom.2012.10.142

Papry, R.I., Fujisawa, S., Zai, Y., Akhyar, O., Mashio, A.S., Hasegawa, H., 2021. Freshwater phytoplankton: Salinity stress on arsenic biotransformation. Environ. Pollut. 270, 116090. https://doi.org/10.1016/j.envpol.2020.116090

Papry, R.I., Miah, S., Hasegawa, H., 2022. Integrated environmental factor-dependent growth and arsenic biotransformation by aquatic microalgae: A review. Chemosphere 303, 135164. https://doi.org/10.1016/j.chemosphere.2022.135164

Pietrini, F., Iannelli, M.A., Pasqualini, S., Massacci, A., 2003. Interaction of Cadmium with Glutathione and Photosynthesis in Developing Leaves and Chloroplasts of Phragmites australis (Cav.) Trin. ex Steudel. Plant Physiol. 133, 829–837. https://doi.org/10.1104/pp.103.026518

Polle, J.E.W., Kanakagiri, S., Jin, E., Masuda, T., Melis, A., 2002. Truncated chlorophyll antenna size of the photosystems—a practical method to improve microalgal productivity and hydrogen production in mass culture. Int. J. Hydrog. Energy, BIOHYDROGEN 2002 27, 1257–1264. https://doi.org/10.1016/S0360-3199(02)00116-7

Portis, A.R., 2003. Rubisco activase – Rubisco's catalytic chaperone. Photosynth. Res. 75, 11–27. https://doi.org/10.1023/A:1022458108678

Rathi, B.S., Kumar, P.S., 2021. A review on sources, identification and treatment strategies for the removal of toxic Arsenic from water system. J. Hazard. Mater. 418, 126299. https://doi.org/10.1016/j.jhazmat.2021.126299

Ryan-Keogh, T.J., Thomalla, S.J., 2020. Deriving a Proxy for Iron Limitation From Chlorophyll Fluorescence on Buoyancy Gliders. Front. Mar. Sci. 7, 275. https://doi.org/10.3389/fmars.2020.00275

Samanta, S., Banerjee, A., Roychoudhury, A., 2022. Arsenic Toxicity is Counteracted by Exogenous Application of Melatonin to Different Extents in Arsenic-susceptible and Arsenic-tolerant Rice Cultivars. J. Plant Growth Regul. 41, 2210–2231. https://doi.org/10.1007/s00344-021-10432-0

Schallenberg, C., Strzepek, R.F., Schuback, N., Clementson, L.A., Boyd, P.W., Trull, T.W., 2020. Diel quenching of Southern Ocean phytoplankton fluorescence is related to iron limitation. Biogeosciences 17, 793–812. https://doi.org/10.5194/bg-17-793-2020

Schuback, N., Flecken, M., Maldonado, M.T., Tortell, P.D., 2016. Diurnal variation in the coupling of photosynthetic electron transport and carbon fixation in iron-limited phytoplankton in the NE subarctic Pacific. Biogeosciences 13, 1019–1035. https://doi.org/10.5194/bg-13-1019-2016

Schuback, N., Schallenberg, C., Tortell, P.D., 2020. Non-photochemical quenching of chl-a fluorescence: an undervalued optical indicator of photosynthetic efficiency. https://doi.org/10.13140/RG.2.2.31978.26569

Schuback, N., Tortell, P.D., Berman-Frank, I., Campbell, D.A., Ciotti, A., Courtecuisse, E., Erickson, Z.K., Fujiki, T., Halsey, K., Hickman, A.E., Huot, Y., Gorbunov, M.Y., Hughes, D.J., Kolber, Z.S., Moore, C.M., Oxborough, K., Prášil, O., Robinson, C.M., Ryan-Keogh, T.J., Silsbe, G., Simis, S., Suggett, D.J., Thomalla, S., Varkey, D.R., 2021a. Single-Turnover Variable Chlorophyll Fluorescence as a Tool for Assessing Phytoplankton Photosynthesis and Primary Productivity: Opportunities, Caveats and Recommendations. Front. Mar. Sci. 8, 690607. https://doi.org/10.3389/fmars.2021.690607

Schuback, N., Tortell, P.D., Berman-Frank, I., Campbell, D.A., Ciotti, A., Courtecuisse, E., Erickson, Z.K., Fujiki, T., Halsey, K., Hickman, A.E., Huot, Y., Gorbunov, M.Y., Hughes, D.J., Kolber, Z.S., Moore, C.M., Oxborough, K., Prášil, O., Robinson, C.M., Ryan-Keogh, T.J., Silsbe, G., Simis, S., Suggett, D.J., Thomalla, S., Varkey, D.R., 2021b. Single-Turnover Variable Chlorophyll Fluorescence as a Tool for Assessing Phytoplankton Photosynthesis and Primary Productivity: Opportunities, Caveats and Recommendations. Front. Mar. Sci. 8.

Serre-Fredj, L., Jacqueline, F., Navon, M., Izabel, G., Chasselin, L., Jolly, O., Repecaud, M., Claquin, P., 2021. Coupling high frequency monitoring and bioassay experiments to investigate a harmful algal bloom in the Bay of Seine (French-English Channel). Mar. Pollut. Bull. 168, 112387. https://doi.org/10.1016/j.marpolbul.2021.112387

Suresh Kumar, K., Dahms, H.-U., Lee, J.-S., Kim, H.C., Lee, W.C., Shin, K.-H., 2014. Algal photosynthetic responses to toxic metals and herbicides assessed by chlorophyll a fluorescence. Ecotoxicol. Environ. Saf. 104, 51–71. https://doi.org/10.1016/j.ecoenv.2014.01.042

Tlili, S., Ovaert, J., Souissi, A., Ouddane, B., Souissi, S., 2016. Acute toxicity, uptake and accumulation kinetics of nickel in an invasive copepod species: Pseudodiaptomus marinus. Chemosphere 144, 1729–1737. https://doi.org/10.1016/j.chemosphere.2015.10.057

Ünlü, C., Drop, B., Croce, R., van Amerongen, H., 2014. State transitions in Chlamydomonas reinhardtii strongly modulate the functional size of photosystem II but not of photosystem I. Proc. Natl. Acad. Sci. 111, 3460–3465. https://doi.org/10.1073/pnas.1319164111

Wang, S., Wang, Y., Liang, Y., Cao, W., Sun, C., Ju, P., Zheng, L., 2020. The interactions between microplastic polyvinyl chloride and marine diatoms: Physiological, morphological, and growth effects. Ecotoxicol. Environ. Saf. 203, 111000. https://doi.org/10.1016/j.ecoenv.2020.111000

Wang, Z., Gui, H., Luo, Z., Sarakiotia, I.L., Yan, C., Laing, G.D., 2020. Arsenic release: Insights into appropriate disposal of arsenic-loaded algae precipitated from arsenic contaminated water. J. Hazard. Mater. 384, 121249. https://doi.org/10.1016/j.jhazmat.2019.121249

Xiao, X., Tong, Y., Wang, D., Gong, Y., Zhou, Z., Liu, Y., Huang, H., Zhang, B., Li, H., You, J., 2022. Spatial distribution of benthic toxicity and sediment-bound metals and arsenic in Guangzhou urban waterways: Influence of land use. J. Hazard. Mater. 439, 129634. https://doi.org/10.1016/j.jhazmat.2022.129634

Zhang, Huihui, Liu, X., Zhang, Hongbo, Wang, Y., Li, T., Che, Y., Wang, J., Guo, D., Sun, G., Li, X., 2021. Thioredoxin-like protein CDSP32 alleviates Cd-induced photosynthetic inhibition in tobacco leaves by regulating cyclic electron flow and excess energy dissipation. Plant Physiol. Biochem. 167, 831–839. https://doi.org/10.1016/j.plaphy.2021.09.016

Zhang, W., Miao, A.-J., Wang, N.-X., Li, C., Sha, J., Jia, J., Alessi, D.S., Yan, B., Ok, Y.S., 2022. Arsenic bioaccumulation and biotransformation in aquatic organisms. Environ. Int. 163, 107221. https://doi.org/10.1016/j.envint.2022.107221

Zhu, Z., Wu, Y., Xu, J., Beardall, J., 2019. High copper and UVR synergistically reduce the photochemical activity in the marine diatom Skeletonema costatum. J. Photochem. Photobiol. B 192, 97–102. https://doi.org/10.1016/j.jphotobiol.2019.01.016

Zidour, M., Boubechiche, Z., Pan, Y.-J., Bialais, C., Cudennec, B., Grard, T., Drider, D., Flahaut, C., Ouddane, B., Souissi, S., 2019. Population response of the estuarine copepod Eurytemora affinis to its bioaccumulation of trace metals. Chemosphere 220, 505–513. https://doi.org/10.1016/j.chemosphere.2018.12.148

Zong, X., Zhang, J., Zhu, J., Zhang, L., Jiang, L., Yin, Y., Guo, H., 2021. Effects of polystyrene microplastic on uptake and toxicity of copper and cadmium in hydroponic wheat seedlings (Triticum aestivum L.). Ecotoxicol. Environ. Saf. 217, 112217. https://doi.org/10.1016/j.ecoenv.2021.112217

Zsiros, O., Nagy, G., Patai, R., Solymosi, K., Gasser, U., Polgár, T.F., Garab, G., Kovács, L., Hörcsik, Z.T., 2020. Similarities and Differences in the Effects of Toxic Concentrations of Cadmium and Chromium on the Structure and Functions of Thylakoid Membranes in Chlorella variabilis. Front. Plant Sci. 11.

Credit author statement

Shagnika Das: Performed the experiment, analysis and drafted the manuscript.

Fabrice Lizon : Supervised the physiological measurements and analyses. Reviewed and helped in drafting the manuscript.

Francois Gevaert : Analyzed the pigment concentrations, reviewed the manuscript.

Capucine Bialais: Helped during experiments.

Gwendoline Duong: Performed the analyses in HPLC for pigments.

Baghdad Ouddane: Performed heavy metals analyses.

Sami Souissi: Conceived the project and reviewed the manuscript.

All co-authors: read and commented on the Manuscript.

Declaration of interests

☒The authors declare that they have no known competing financial interests or personal relationships that could have appeared to influence the work reported in this paper.

☐The authors declare the following financial interests/personal relationships which may be considered as potential competing interests:

Environmental implication

Arsenic is ubiquitous and hazardous to human health in trace amounts, given the dreadful record of lethal cases from arsenic contamination, worldwide. Hence, new tools are warranted for this compelling necessity to monitor effects of arsenic in nature. This study proposes new indicators of arsenic contamination through physiology of a microalgae (*Diacronema lutheri*) using variable fluorescence. Furthermore, a linkage of physiological markers with ecotoxicology using non-destructive, rapid and a precise method is reported. A strong correlation of variable fluorescence and growth parameters exemplified the precision of the proposed indicators. Such rapid, non-polluting, novel techniques are advantageous to environmental risk assessors.

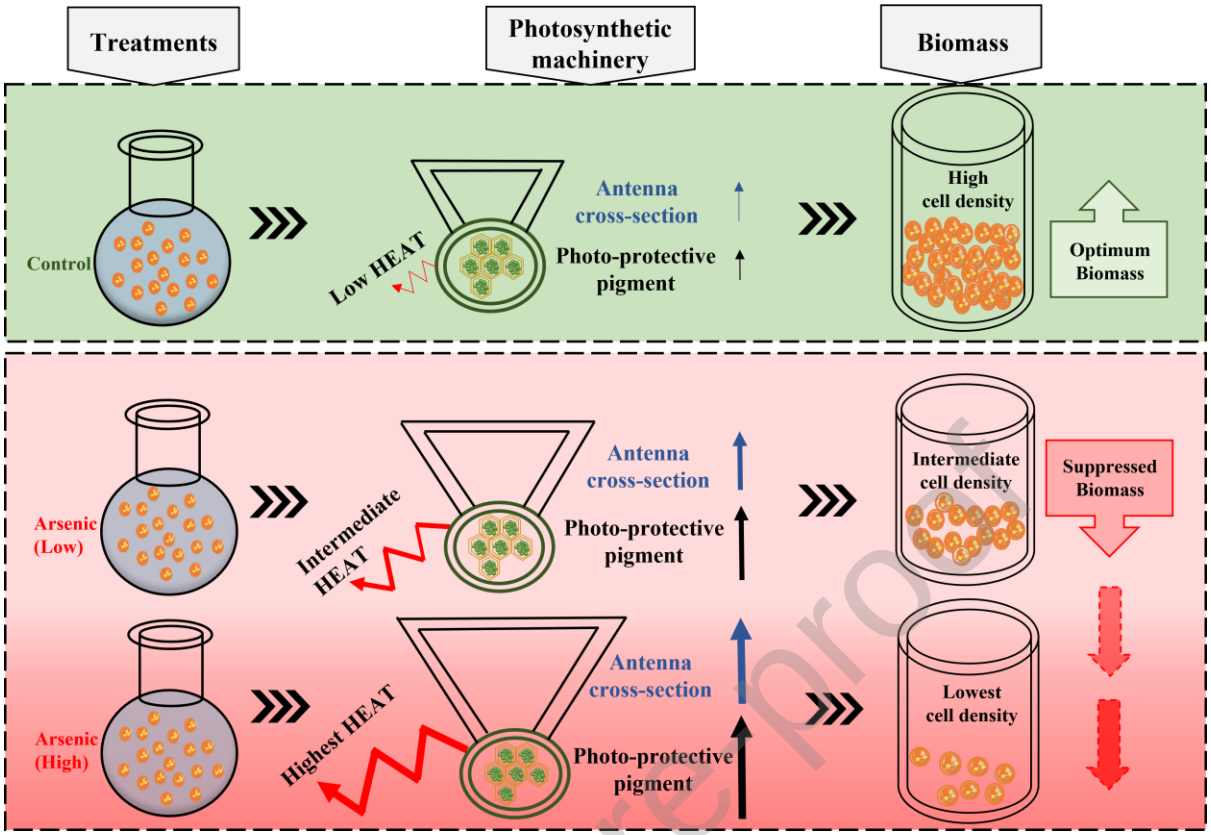

Highlights-

6. Arsenic (As) enhanced photoprotective processes and restricted biomass production.
7. Optical and functional absorption cross-section are useful indicators of As toxicity.
8. Non-photochemical quenching (NPQ-NSV) positively correlated to de-epoxidation ratio.
9. Significant affinity between Fe and As bioaccumulation by *D. lutheri* was observed.
10. Variable fluorescence endorsed an easy and compliant method to show As toxicity.